

Journal of Biomedical Optics

SPIEDigitalLibrary.org/jbo

Measurement of anisotropic reflection of flowing blood using optical coherence tomography

Kweon-Ho Nam
Bosu Jeong
In Oh Jung
Hojin Ha
Ki Hean Kim
Sang Joon Lee

Measurement of anisotropic reflection of flowing blood using optical coherence tomography

Kweon-Ho Nam,^{a,*} Bosu Jeong,^{b,*} In Oh Jung,^c
Hojin Ha,^c Ki Hean Kim,^{c,d} and Sang Joon Lee^{a,b,c,d}

^aPohang University of Science and Technology, Center for Biofluid and Biomimic Research, San 31, Hyoja-dong, Nam-gu, Pohang, Gyeongbuk 790-784, Republic of Korea

^bPohang University of Science and Technology, School of Interdisciplinary Bioscience and Bioengineering, San 31, Hyoja-dong, Nam-gu, Pohang, Gyeongbuk 790-784, Republic of Korea

^cPohang University of Science and Technology, Department of Mechanical Engineering, San 31, Hyoja-dong, Nam-gu, Pohang, Gyeongbuk 790-784, Republic of Korea

^dPohang University of Science and Technology, Division of Integrative Biosciences and Biotechnology, San 31, Hyoja-dong, Nam-gu, Pohang, Gyeongbuk 790-784, Republic of Korea

Abstract. Light reflectance of blood is a complex phenomenon affected by hematocrit and red blood cell (RBC) aggregation (rouleaux formation). According to the hypothesis that RBC rouleaux are aligned with the direction of blood flow, the spatial alignment of RBC rouleaux, as well as their size and quantity in the blood, may also affect light reflectance. The present study aims to investigate the effect of the spatial alignment and distribution of RBC rouleaux on light reflection using optical coherence tomography (OCT). Blood flow velocity and reflectance profiles in a rat jugular-femoral bypass loop were simultaneously measured using a Doppler swept-source OCT system at various incident angles from -30 to $+30$ deg. The reflectance profiles of flowing blood show nonmonotonous decay with a local negative peak at the center of the tube. The profiles vary depending on the incident angle. This angular dependence is stronger at a higher angle of incidence. The anisotropic reflectance of flowing blood is consistent with the hypothesis on the spatial alignment of RBC rouleaux. © 2011 Society of Photo-Optical Instrumentation Engineers (SPIE). [DOI: 10.1117/1.3660299]

Keywords: optical coherence tomography; red blood cell aggregation; reflectance anisotropy.

Paper 11450LRR received Aug. 21, 2011; revised manuscript received Oct. 20, 2011; accepted for publication Oct. 24, 2011; published online Nov. 22, 2011.

Light reflectance or transmission measurement has been commonly used to quantify the level of red blood cell (RBC) aggregation.¹ However, conventional photometric methods do not provide the information about a depth-intensity relationship but only measure the total light intensity transmitted through or reflected from the blood. Optical coherence tomography (OCT)

has been suggested as a promising modality for measuring RBC aggregation in submillimeter-sized blood vessels because OCT has high spatial resolution. Although most of the OCT measurements of RBC aggregation have been performed to study optical clearing² or to noninvasively measure hematocrit,³ based on the fact that the increase of RBC aggregation reduces light scattering and enhances light transmission, it may be possible to estimate RBC aggregation by analyzing the OCT depth reflectance profile. In addition, the reflectance profile may imply the information about the spatial alignment of RBC rouleaux in flowing blood as hypothesized in previous studies.^{4,5} According to this hypothesis, RBC rouleaux are aligned in a cone-shape with a tilted orientation at the central region of large-diameter tubes as schematized in Fig. 1(a).

The objective of the present study is to evaluate the feasibility of OCT intensity imaging in investigating the orientation of RBC rouleaux and their spatial distribution in a submillimeter-scale tube. *In situ* measurements were performed in a rat jugular-femoral bypass loop. Variation of OCT depth reflectance profile of blood under static and flowing conditions and its dependence on the incident angle of OCT illumination were obtained and discussed.

The OCT system employed in a previous study⁶ was adopted to acquire blood reflectivity images and velocity information [Fig. 1(b)]. The OCT system used a custom-built wavelength-swept source with a polygon wavelength filter and a semiconductor optical amplifier as a gain medium. The wavelength-swept source had a central wavelength of 1312 nm and a bandwidth of 107 nm. The sweeping rate and the output power were 47.6 kHz and 45 mW, respectively. The measured sensitivity of the OCT system was 107 dB. The image resolutions were 8 and 20 μm in the air in the axial and lateral directions, respectively. These were determined by measuring the full width at half maximum intensity of a mirror image, and as the width of the Gaussian beam waist. Lateral scanning was performed at a rate of 95.2 frames/s during measurements using 500 A-scans over 800 μm with $\times 12.5$ oversampling. An OCT intensity image was obtained by squaring the measured interference spectrum. Blood flow velocities were calculated from the phase difference between two successive A-lines by assuming a constant refractive index of 1.38.

To avoid measurement difficulty and inaccuracy caused by tissue motion from breathing and heart beating *in vivo*, as well as the possible deformation of RBC rouleaux in *in vitro* experiments, a rat jugular-femoral bypass loop model was used in the current study. An 8-week old male Sprague-Dawley rat was anesthetized with an intramuscular injection of ketamine (100 mg/kg) and xylazine (10 mg/kg). A heparin-filled PE-50 catheter (ID = 0.58 mm, OD = 0.965 mm, Intramedic polyethylene tubing, Becton Dickinson, Sparks, Maryland) with a length of 50 cm was cannulated into the right jugular vein, and the other end of the tube was inserted into the left femoral artery. The middle part of the jugular-femoral bypass loop was straightened and placed horizontally on a manual goniometer. The angle of incidence varied from -30 to $+30$ deg at an interval of 10 deg by adjusting the goniometer (Fig. 1). Cross-sectional

*Contributed equally to this work.

Address all correspondence to: Sang Joon Lee and Ki Hean Kim, Pohang University of Science and Technology, POSTECH, Department of Mechanical Engineering, San 31, Hyoja-dong, Pohang, 790-784 Republic of Korea; Tel: 82542792169; Fax: 82542793199; E-mail: sjlee@postech.ac.kr and kiheankim@postech.ac.kr.

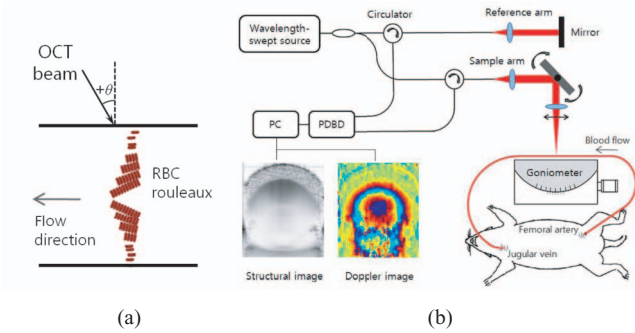


Fig. 1 Experimental setup. (a) Schematic representation of the hypothesized alignment of RBC rouleaux across the tube, where θ denotes the angle of incidence from a line perpendicular to the flow direction. (b) Schematic diagram of the OCT system and the rat jugular-femoral bypass model (PC: personal computer; PDBD: polarization-diverse balanced detection).

OCT images were acquired at each incident angle for further analysis.

Figure 2(a) shows the variation of centerline blood velocity during a cardiac cycle in a rat jugular-femoral bypass loop at an incident angle of 10 deg and the velocity profiles at systole and diastole are shown in Fig. 2(b). The systolic and diastolic velocities were 9.1 and 5.2 cm/sec at the center of the tube, respectively. No reverse flow was observed because there was no

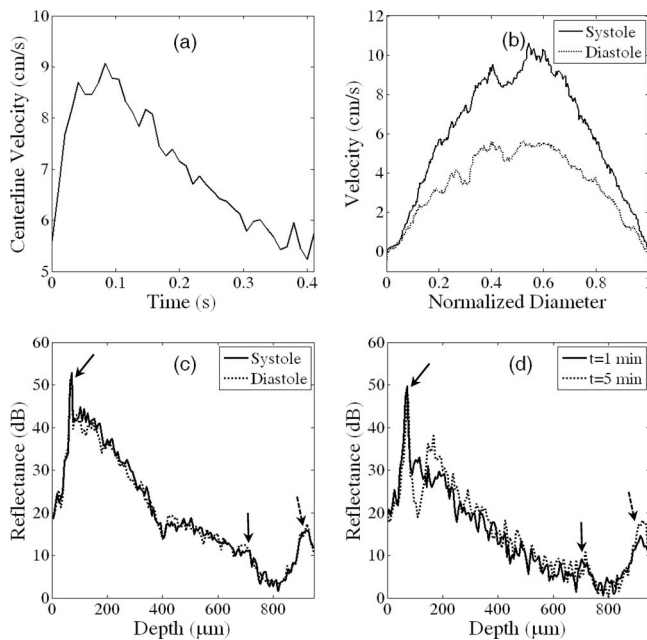


Fig. 2 OCT measurements of blood flow and depth reflectance. (a) Temporal variation of flow velocity at the center of the rat jugular-femoral bypass loop during a cardiac cycle. (b) Velocity profiles at systole and diastole. (c) OCT depth reflectance profiles of blood at systolic and diastolic phases, and (d) reflectance profiles at 1 and 5 min after the complete stoppage of blood flow. The solid and dashed arrows in (c) and (d) represent the inner and outer boundaries of the tube, respectively. All the measurements were performed at the incident angle of 10 deg.

peripheral vascular resistance in the bypass model. The velocity profiles were the same regardless of the incident angle.

The A-lines across the center of the tube in the two-dimensional OCT images were used to obtain depth reflectance profiles instead of M-scans. This is because M-mode scanning requires precise alignment of the OCT sample beam and the tube centerline to avoid intermeasurement variability. Typical OCT depth reflectance profiles at the systolic and diastolic phases are shown in Fig. 2(c). As can be seen, OCT reflectance decreased with penetration depth due to light attenuation in the blood. A local negative peak was observed in the central region. The negative peak resulted from high RBC aggregation because a low shear rate in the central region facilitates the formation of RBC rouleaux. The slope of depth reflectance and the amplitude of the negative peak in the central region did not significantly vary during a cardiac cycle at the same incident angle. The differences in OCT depth reflectance at systolic and diastolic phases were less than about 1 dB at all incident angles ranging from -30 to $+30$ deg. A complete stoppage of blood flow by clamping the bypass loop with a hemostatic forceps caused a significant decrease in the slope of depth reflectance [$t = 1$ min in Fig. 2(d)], and the negative peak at the tube center disappeared. These phenomena can be explained by the overall increase of RBC aggregation level inside the tube under static condition.⁷ After 5 min from the flow stoppage, a low-reflectance layer appeared on top of the blood due to the sedimentation of RBCs [Fig. 2(d)].

To investigate the effects of the incident angle on OCT depth reflectance in flowing blood, cross-sectional OCT images were taken at six different incident angles from -30 to $+30$ deg. At each incident angle, a total of 300 OCT images during eight cardiac cycles were obtained and averaged. The A-lines across the tube center were used to calculate depth reflectance. The results at incident angles of -20 and $+20$ deg are shown in Fig. 3(a). With the assumption that RBCs do not aggregate at a high shear rate along the nearest wall region,⁴ initial reflectance was set to 0 dB. OCT reflectance decreased linearly in the top area showing the same slope at both incidence angles. As the penetration depth increased, declination of reflectance became greater at $+20$ deg. A significant difference in reflectance at the two opposite angles was observed in the central region, with a difference (ΔR) of approximately 5 dB. ΔR increased in

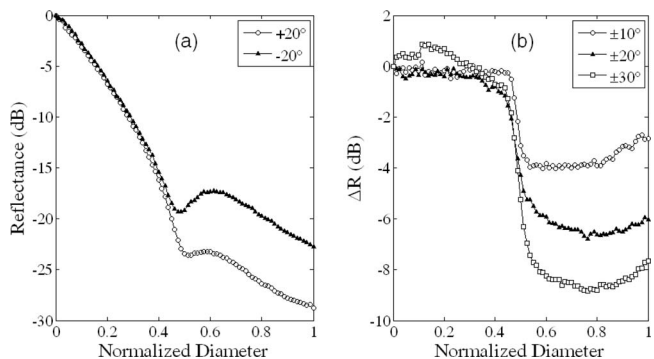


Fig. 3 Incident angle dependence of OCT reflectance as a function of diameter. (a) OCT depth reflectance profiles averaged over eight cardiac cycles at the incident angles of ± 20 deg. (b) Comparison of the depth reflectance difference (ΔR) between the same incident angles with opposite directions ($\Delta R = R_{\text{positive angle}} - R_{\text{negative angle}}$).

proportion to the angle of incidence, which was mostly caused by the variations in the central area of the tube as shown in Fig. 3(b). Since the angle of incidence affects reflection loss of light on the tube surface and depth of blood layer, only ΔR between the same incidence angles at opposite directions was calculated in this study. OCT reflectance was observed to be higher at negative (or lower at positive) angles of incidence throughout the measurement range, and ΔR was found to be dependent on the magnitude of the incident angle. Based on the hypothetical model in Fig. 1(a) and the experimental results in Fig. 3, it can be conjectured that RBC rouleaux aligned more perpendicular to the OCT beam have a larger scattering cross-section compared to those aligned less perpendicular to the OCT beam.

It has been known that multiple scattering leads to nonsingle exponential decay of OCT depth reflectance.^{8,9} Since whole blood contains highly dense scatters (RBCs), the multiple scattering from RBCs may cause the OCT signals at both boundaries to have an unequal slope as shown in Figs. 2(c) and 3(a). According to the hypothesized model depicted in Fig. 1(a), the size of RBC rouleaux in flowing blood is increased with approaching the tube center and their orientation is symmetric about the tube axis. In this case, the OCT beams having the same incident angle in the opposite directions travel different paths. Assuming a single scattering model, the reflectance difference ΔR is expected to be zero at both walls due to their symmetric travel path. However, for the multiple scattering in whole blood, the combined effects of the nonsingle exponential decay of OCT depth reflectance and the anisotropic scattering of RBC rouleaux caused by the different orientation along the depth direction may result in the reflectance difference at the far-side boundary as shown in Fig. 3.

Other effects, such as alignment of individual RBCs and RBC density variation caused by inertial migration, may affect the OCT depth reflectance. However, the evidence of inertial migration was not observed in the present results. This may result from the relatively large diameter (580 μm) of the bypass loop tested in this study, which is supported by the results of a previous study performed with flow cells of two different widths, 2 and 0.2 mm.⁹ Individual RBCs may align under a well-controlled steady flow condition and this may affect the OCT reflectance in a near wall region. Although it is doubtful whether this phenomenon occurs under pulsatile flow in our flow model, we cannot completely rule out the possibility.

We suggest that OCT intensity imaging is a useful modality for investigating characteristic behavior of RBC rouleaux in submillimeter-scale blood vessels using the anisotropic nature of OCT depth reflectance in flowing blood. Further studies will be necessary to better understand the mechanisms of anisotropic reflectance of OCT in flowing blood.

Acknowledgments

This work was supported by the Creative Research Initiatives (Diagnosis of Biofluid Flow Phenomena and Biomimic Research) of the Ministry of Education, Science, and Technology/National Research Foundation (MEST/NRF) of Korea. This research was also supported in part by the National Research Foundation Grant (Nos. 2010-0028014 and 2010-0014874) and World Class University (WCU) program through the National Research Foundation of Korea funded by the Ministry of Education, Science and Technology (R31-2008-000-10105-0).

References

1. O. K. Baskurt, M. Uyuklu, M. R. Hardeman, and H. J. Meiselman, "Photometric measurements of red blood cell aggregation: light transmission versus light reflectance," *J. Biomed. Opt.* **14**(5), 054044 (2009).
2. V. V. Tuchin, X. Xu, and R. K. Wang, "Dynamic optical coherence tomography in studies of optical clearing, sedimentation, and aggregation of immersed blood," *Appl. Opt.* **41**(1), 258–271 (2002).
3. X. Xu, L. Yu, and Z. Chen, "Effect of erythrocyte aggregation on hematocrit measurement using spectral-domain optical coherence tomography," *IEEE Trans. Biomed. Eng.* **55**(12), 2753–2758 (2008).
4. D. G. Paeng, R. Y. Chiao, and K. K. Shung, "Echogenicity variations from porcine blood II: the "bright ring" under oscillatory flow," *Ultrasound Med. Biol.* **30**(6), 815–825 (2004).
5. L. Allard, G. Cloutier, and L. G. Durand, "Effect of theinsonification angle on the Doppler backscattered power under red blood cell aggregation conditions," *IEEE Trans. Ultrason. Ferroelectr. Freq. Control* **43**(2), 211–219 (1996).
6. B. Jeong, B. Lee, M. S. Jang, H. Nam, S. J. Yoon, T. Wang, J. Doh, B. G. Yang, M. H. Jang, and K. H. Kim, "Combined two-photon microscopy and optical coherence tomography using individually optimized sources," *Opt. Express* **19**(14), 13089–13096 (2011).
7. K. H. Nam, D. G. Paeng, and M. J. Choi, "Ultrasonic backscatter from rat blood in aggregating media under *in vitro* rotational flow," *IEEE Trans. Ultrason. Ferroelectr. Freq. Control* **56**(2), 270–279 (2009).
8. J. Kalkman, A. V. Bykov, D. J. Faber, and T. G. van Leeuwen, "Multiple and dependent scattering effects in Doppler optical coherence tomography," *Opt. Express* **18**(4), 3883–3892 (2010).
9. D. P. Popescu and M. G. Sowa, "Characteristics of time-domain optical coherence tomography profiles generated from blood-saline mixtures," *Phys. Med. Biol.* **54**(15), 4759–4775 (2009).